AD_____

Award Number: DAMD17-98-1-8583

TITLE: Unique G-Rich Oligonucleotides Which Inhibit the Growth of Prostatic Carcinoma Cells

PRINCIPAL INVESTIGATOR: Donald M. Miller, M.D., Ph.D.
Paula J. Bates, Ph.D.
John O. Trent, Ph.D.

CONTRACTING ORGANIZATION: University of Louisville
Louisville, Kentucky 40292

REPORT DATE: July 2002

TYPE OF REPORT: Annual

PREPARED FOR: U.S. Army Medical Research and Materiel Command
Fort Detrick, Maryland 21702-5012

REPORT DOCUMENTATION PAGE

Form Approved
OMB No. 074-0188

1. AGENCY USE ONLY (Leave blank)	2. REPORT DATE	3. REPORT TYPE AND DATES COVERED
	July 2002	Annual (1 Jul 01 - 30 Jun 02)

4. TITLE AND SUBTITLE
Unique G-Rich Oligonucleotides Which Inhibit the Growth of Prostatic Carcinoma Cells

5. FUNDING NUMBERS
DAMD17-98-1-8583

6. AUTHOR(S)
Donald M. Miller, M.D., Ph.D.
Paula J. Bates, Ph.D.
John O. Trent, Ph.D.

7. PERFORMING ORGANIZATION NAME(S) AND ADDRESS(ES)
University of Louisville
Louisville, Kentucky 40292

E-Mail: dkkonz01@louisville.edu

8. PERFORMING ORGANIZATION REPORT NUMBER

9. SPONSORING / MONITORING AGENCY NAME(S) AND ADDRESS(ES)
U.S. Army Medical Research and Materiel Command
Fort Detrick, Maryland 21702-5012

10. SPONSORING / MONITORING AGENCY REPORT NUMBER

11. SUPPLEMENTARY NOTES
report contains color

12a. DISTRIBUTION / AVAILABILITY STATEMENT
Approved for Public Release; Distribution Unlimited

12b. DISTRIBUTION CODE

13. Abstract ***(Maximum 200 Words)*** *(abstract should contain no proprietary or confidential information)*
G-rich oligonucleotides (GROs) are a novel class of non-antisense nucleic acids that exhibit potent antiproliferative effects against malignant cells, including prostate cancer cells. The mechanism of GRO antiproliferative activity depends on their binding to nucleolin protein. Because they work by a novel mechanism (different from antisense oligonucleotides or traditional chemotherapy agents) and are expected to have few side effects, they have promise as new therapeutic agents for the treatment of prostate cancer. The major aims of this study were to test the efficacy of GROs in inhibiting the growth and metastasis of prostate cancer in rodent models, to investigate the mechanism of GROs, and to develop structural models of nucleolin for the development of new inhibitors. In the first year of this study, we have optimized GRO formulation and delivery *in vitro* and *in vivo*, and have been able to demonstrate impressive inhibitory effects against an aggressive hormone-independent tumor (DU145) in mice. We have also examined the effect of combined GRO and chemotherapy treatment on prostate cancer cells, and made considerable progress in developing a structural model of nucleolin. In summary, our results so far strongly support the potential of GROs as novel therapeutic agents for prostate cancer. Our work during this period has resulted in peer-reviewed publication and a patent filing.

14. SUBJECT TERMS	15. NUMBER OF PAGES
experimental therapeutics, oligonucleotides, prostate cancer, animal models, nucleolin, G-quartets, quadruplex, non-antisense	23
	16. PRICE CODE

17. SECURITY CLASSIFICATION OF REPORT	18. SECURITY CLASSIFICATION OF THIS PAGE	19. SECURITY CLASSIFICATION OF ABSTRACT	20. LIMITATION OF ABSTRACT
Unclassified	Unclassified	Unclassified	Unlimited

Table of Contents

INTRODUCTION

The proposed research was based on our discovery of novel G-rich oligonucleotides (GROs) that have antiproliferative activity against prostate cancer and other malignant cell lines (1). Previously, we had demonstrated that the biological activity of GROs was correlated with their ability to bind to a multifunctional cellular protein called nucleolin (1). Therefore, we postulated that these oligonucleotides work by a novel non-antisense mechanism that involves nucleolin binding. The major goal of this study was to evaluate the therapeutic potential of GROs by investigating their ability to inhibit tumor growth and metastasis in rodent models of prostate cancer. Experiments to examine the mechanism of GRO activity and to develop novel nucleolin-binding agents were also proposed

BODY

The progress on each task outlined in the Statement of Work is detailed below:

Task 1: To examine the relationship between levels of nucleolin/GRO binding protein, the rate of cell proliferation, and sensitivity to GRO effects, using a variety of prostate cell lines (*months 1-6*):

- *a.* establish cell cultures and carry out dose-response studies using GRO29A to determine GI_{50} values for a variety of malignant and immortalized prostate cell lines (*months 1-3*)
- *b.* prepare large cell cultures and extract nuclear, cytoplasmic and plasma membrane proteins (*months 4-5*)
- *c.* southwestern and western blots of extracts (*month 5*)
- *d.* immunofluorescence to examine intracellular and cell surface nucleolin in different cell lines (*month 5-6*)

Progress: Because only a few human prostate cancer lines are available from ATCC (American Type Culture Collection), we chose to take a slightly modified approach to address this aim. The NCI (National Cancer Institute) 60 cell lines panel is a collection of well-characterized human cell lines derived from different malignancies. We submitted GRO26B (a slightly more active analog of GRO29A) for screening against this cell line panel. This oligonucleotide showed cytostatic activity in about one third of the cell lines, including those derived from prostate cancer, leukemia, lung cancer, colon cancer, melanoma, renal cancer, and breast cancer. Both of the prostate cancer cell lines in the panel (DU145 and PC-3) were sensitive to the effects of GRO26B. We have now received cell pellets from each of these cell lines and will proceed to prepare nuclear and S-100 extracts from these in order to detect nuclear and plasma membrane GRO binding protein/nucleolin by southwestern and western blotting. This approach will allow us to determine if there is a correlation between levels of nucleolin and GRO sensitivity (GI_{50} calculated from NCI60 screening data) in a much larger number of cell lines than originally proposed. Examination of cell surface nucleolin by immunofluorescence has led to some important data that suggest that nucleolin levels may be higher in the plasma membrane and cytoplasm of cancer cells compared to normal cells. Figure 1A shows that indirect fluorescent staining of non-permeabilized cells using a nucleolin monoclonal antibody indicates high levels of nucleolin in the plasma membrane (some staining is also seen in the cytoplasm) of cancer cells (especially prostate cancer cells, DU145), but undetectable levels in normal skin cells (HS27). This method of staining is much more selective for malignant cells than nuclear nucleolin (Figure 1B), and may represent a novel method to detect malignant cells.

Task 2: To optimize the delivery of oligonucleotides to tumor cells in culture and *in vivo* (*months 1-16*):

a. obtain or prepare transfection reagents (*months 1-2*)
b. determine uptake of FITC-labeled GRO29A (*months 2-3*)
c. determine activity of GRO29A in cultured cells with different delivery methods (*month 4*)
d. carry out delivery studies in nude mice (9 total) with s.c. DU145 xenografts using internally radiolabeled GRO29A (*months 5-6*)
e. obtain Dunning rat tumor tissue and establish rat model (6 rats) (*months 9-12*)
f. carry out delivery studies in rats (9 total) with s.c. tumors (*months 13-16*)

Progress: The majority of this task has been completed. We assessed several methods (including lipids, lipofectin, streptolysin O) for delivering GRO to cultured cells and found that activity was not increased compared to direct addition of the oligonucleotide to the medium. This is in sharp contrast to most antisense oligonucleotides, which are very poorly internalized in the absence of transfection reagents. In light of these results, we carried out more extensive studies on the uptake of fluorescently labeled oligonucleotides. Figure 2A shows that G-rich oligonucleotides that can bind to nucleolin (GRO26B and PS26B) are very efficiently taken up into the nucleus of DU145 prostate cancer cells whereas unstructured, C-rich, and control G-rich oligonucleotides that have no activity (MIX, PS-MIX, CRO, 15B) show very little uptake. To test the hypothesis that G-quartet formation is responsible for this enhanced uptake we compared the internalization of an active GRO that had been annealed in potassium buffer (which stabilizes G-quartets) or sodium buffer. Figure 2B shows that annealing in potassium did indeed increase the uptake of GROs and also enhanced their antiproliferative activity (not shown). We have not yet carried out the experiments to determine the distribution of radiolabeled oligonucleotides in animals. However, we have determined in preliminary experiments that intraperitoneal (i.p.) injection could inhibit xenograft growth, whereas intratumoral injection resulted in local growth inhibition at the injection site but had no effect on overall tumor volume. Because intravenous injection is an impractical option for studies using large numbers of nude mice, we opted to proceed with the *in vivo* experiments using i.p. injection of GRO. In addition to the studies outlined above, we also compared the stability and antiproliferative activity of GROs with modified backbones in order to determine the optimal oligonucleotide for clinical development (2). These studies, which compare GRO29A (3'-amine modified phosphodiester oligonucleotide) with analogs having phosphodiester (DNA), phosphorothioate (PS), 2'-O-methyl RNA (MR), and mixed backbones, have been recently published in *Biochemistry* (reprint attached). The key results are summarized below:

- Antiproliferative activity for analogs with DNA, PS, but not MR backbones
- Activity of phosphorothioate oligonucleotides is, in part, non-specific
- All GRO analogs form G-quartets and are stable in biological medium
- Half-life of DNA analog of GRO29A is >120h in serum-containing medium, compared with < 1 h for non-G-quartet DNA
- Antiproliferative activity is correlated with nucleolin binding (MR does not bind)
- Activity depends on recognition of G-quartet grooves (not loops or simple G-quartet motif) and the MR grooves are much shallower than other analogs

In conclusion, the conditions for pursuing preclinical studies have now been defined, namely using an unmodified DNA analog of GRO29A (GRO26B, 5'- GGTGGTGGTGGTTGTGGTGGTGGTGG) that has been pre-annealed in a buffer containing potassium ions.

Task 3: To evaluate the efficacy of GROs in inhibiting prostate cancer growth and metastasis *in vivo* (*months 6-21*):

a. determine efficacy in nude mice (approximately 150 total) with DU145, PC-3 and LNCaP xenografts (*months 7-12*)
b. preliminary experiments (12 nude mice) to establish orthotopically implanted PC-3 model (*months 9-11*)
c. determine efficacy in orthotopically implanted mice (24 total) (*months 12-16*)
d. determine efficacy in Dunning rat model (45 Copenhagen rats) (*months 17-21*)

Progress: Part *a.* of this task has been completed for DU145 xenografts and has indicated very impressive antitumor activity of GROs *in vivo*. In the first experiment, we tested the ability of GRO to inhibit the growth of established xenografts in nude mice. Tumors were established by subcutaneous injection of 10^7 DU145 cells. When tumors were palpable (4 days), mice (6 per group) were treated by i.p. injection of GRO26B resuspended in 100 µl of phosphate buffered saline (PBS) or with PBS alone as control. The first day of treatment (4 days after tumor innoculation) was designated "day 0". Mice were treated every 48 h (except day 6 after the start of treatment) for a further four doses, and were euthanized on day 14. Figure 3A shows that this treatment significantly inhibited xenograft growth (tumor volume estimated using calipers). However, we were aware that pre-annealing oligonucleotides in potassium containing buffer greatly enhanced GRO activity in cultured cells (compared to GRO in PBS). Because we were concerned about the possibly toxic effects of injecting high concentrations of KCl i.p., we carried out a preliminary experiment to compare oligonucleotides annealed in potassium and sodium buffers. Mice were treated as described, and these experiments showed that pre-annealing in KCl enhanced antitumor activity (Figure 3B) and was not acutely toxic to the mice by this administration route. For the next experiment, we pre-annealed GRO26B or its C-rich analog (CRO) as control in a phosphate buffer containing 100 mM KCl. The phosphorothioate analog of GRO26B (PS-GRO) was also tested. Mice were innoculated with DU145 cells as described and treatment began after the appearance of the tumors. Mice (6 per group) received a total of six doses of oligonucleotide by i.p. injection on days 0, 1, 2, 4, 6, and 8. Figure 3C shows that GRO26B (but not control CRO or PS-GRO) could completely inhibit tumor growth and could cause tumor regression at concentrations equivalent to 1 mg/kg at 5 mg/kg (Figure 3C). Table 1 shows that estimated tumor volume (calculated from the tumor diameters, as measured with calipers) and the standard error of the data on day 14.

Table 1: Estimated volume of tumors after treatment with GRO or control oligonucleotides

Treatment	Tumor volume (mm^3)
5 mg/kg CRO (control)	313 ± 163
5 mg/kg GRO26B	80 ± 11
5 mg/kg PS-GRO	280 ± 124
1 mg/kg GRO26B	86 ± 27
Buffer	300 ± 95

We did not observe any significant differences in body weight between different groups of mice, but 3 out of 54 mice died during injection of oligonucleotide (one each from 1 mg/kg PS-GRO, 5 mg/kg PS-

GRO, 1 mg/kg GRO26B). This is likely due to the high concentration of KCl and/or the use of bolus injection of oligonucleotide, which is known to have related toxicities. We anticipate that these toxicities can be easily avoided by the use of intravenous infusion in place of bolus injection and by dialysis of GRO prior to administration (the quadruplex is stable once formed and excess K^+ can be removed).

What is most remarkable about the antitumor activity of GRO26B is that it is observed at such low doses of oligonucleotide. A review of the literature and recent meeting abstracts will reveal that most similar experiments that use antisense oligonucleotides *in vivo* typically require 10-30 mg/kg oligonucleotide for appreciable tumor inhibitory activity (3,4). Certainly, the effective dose here (1 mg/kg) is well below the tolerated dose for other oligonucleotides in humans, and most clinical studies are being carried out using doses of up to 6 mg/kg (5).

Task 4: To evaluate combination GRO-cytotoxic drug therapies for prostate cancer (*months 6-24*):

- *a.* evaluate efficacy of combination treatments in cultured cells, and optimal dose sequence (*months 6-9*)
- *b.* examine effects (cell cycle, apoptosis, nucleolin levels) of combination therapies (*months 10-12*)
- *c.* test synergistic combinations *in vivo* (24 mice) (*months 13-24*)

Progress: Combinations of GRO with cis-platin, taxol, 5-fluorouracil (5-FU), caffeine, vinblastine, mithramycin, and camptothecin have been investigated for their effects against DU145 prostate cancer cells. The results are summarized in Figure 4, and indicate that GRO29A has an additive or synergistic effect with most of the chemotherapy agents tested. These data suggest that GROs would be suitable for clinical use in combination with traditional treatments.

Task 5: To develop homology models of nucleolin and carry out a "virtual screen" of a library of small molecules to identify potential nucleolin inhibitors (*months 1-24*):

- *a.* optimization of preliminary model (*months 1-5*)
- *b.* modeling of nucleolin with GRO29A (*months 6-9*)
- *c.* virtual screen of library of small molecules (*months 6–15*)
- *d.* *in vitro* testing of identified compounds (*months 12-18*)
- *e.* preliminary *in vivo* testing of identified compounds in nude mice (18 mice) (*months 19-24*)
- *f.* rationalization of activity by molecular modeling (*months 16-24*)

Progress: In independent studies (DAMD17-01-1-0067 to Paula Bates), the co-investigator has identified RNA binding domains 1 and 2 (RBD-1,2) of nucleolin as the region that recognizes GROs. Homology models of the nucleolin RNA binding domains 1 and 2 have been successfully created as per Task 5. However, during this grant period the NMR structure of these domains separately and complexed with the nucleolin recognition element, an RNA stem loop structure, were reported (6,7). GRO26B has been computationally docked onto the NMR structure and the orientation is consistent with our structure activity relationship, that is, the loop regions of the GRO are not directly involved in binding to nucleolin (Figure 5).

Figure 5: Model of nucleolin RBD-1,2 binding to GRO26B

KEY RESEARCH ACCOMPLISHMENTS

The following is a list of significant results and achievements:

- Potent inhibition of tumor growth by GRO26B in mouse model of prostate cancer (*Fig.* 3).
- *In vivo* activity of GRO observed as a single agent at much lower doses than antisense (*Fig.* 3).
- Synergistic or additive effects of GRO with chemotherapy drugs in prostate cancer cells (*Fig.* 4).
- Nucleolin-binding GROs have efficient cellular uptake that is enhanced by potassium (*Fig.* 2).
- Nucleolin is present at high levels on the surface of cancer cells but not normal cells (*Fig.* 1).
- Molecular model of nucleolin binding to GRO has been successfully generated and will facilitate virtual screening for nucleolin inhibitors (*Fig.* 5).

REPORTABLE OUTCOMES

Manuscript: The data generated during this reporting period were included in the following:

Dapic V, Bates PJ, Trent JO, Rodger A, Thomas SD, Miller DM. Antiproliferative activity of G-quartet-forming oligonucleotides with backbone modifications. *Biochemistry* 2002, **41**, 3676-3685 (attached).

Abstracts and meeting presentations:

Bates PJ, Trent JO, Miller DM, McGregor W, Burke T, Casson L, Castillos T, Dapic V, Girvan A, Hamhouyia F, Khan D, Mi Y, Sharma V, Thomas S, Xu X. Development of antiproliferative agents targeting nucleolin. Presented at the *American Association of Cancer Research Molecular Targets Conference*, Miami, November 2001. Published in CLINICAL *CANCER RESEARCH* **7**, 157 Suppl. S.

Yingchang Mi, Shelia D. Thomas, Xiaohua Xu, Lavona Casson, Donald M. Miller, Paula J. Bates. Validation of nucleolin as a novel target for cancer drug discovery. Presented at the *American Association of Cancer Research Annual Meeting*, San Francisco, April 2002.

Patent filed:

Bates PJ, Miller DM, Trent JO, Xu X. A New Method for the Diagnosis and Prognosis of Malignant Diseases.

Awards and Honors:

2001 Founders' Medal from the Southern Society of Clinical Investigators awarded to Donald M. Miller, M.D., Ph.D.

CONCLUSIONS

This study was based on promising preliminary data showing that novel non-antisense G-rich oligonucleotides (GROs) have antiproliferative activity against prostate cancer cells in culture. The potential of these GROs as new therapeutic agents has now been established by our current data showing remarkable activity of the lead GRO (GRO26B) in a mouse model of prostate cancer. Providing that the GROs have the anticipated lack of toxicity in animal models, these efficacy results are expected to lead to a human clinical trial of GROs in the near future.

Our discovery that nucleolin is expressed at high levels on the surface of prostate cancer cells, but not on the surface of normal skin cells, confirms our hypothesis that nucleolin is a cancer-selective target for drug discovery. Development of new small molecule nucleolin inhibitors is now in progress based on a molecular model of GRO binding to the relevant domains of nucleolin.

REFERENCES

[1]. Bates PJ, Kahlon JB, Thomas SD, Trent JO, Miller DM. Antiproliferative activity of G-rich oligonucleotides correlates with protein binding (1999), *J. Biol. Chem.* **274,** 26369-26377

[2]. Dapic V, Bates PJ, Trent JO, Rodger A, Thomas SD, Miller DM. Antiproliferative activity of G-quartet-forming oligonucleotides with backbone and sugar modifications (2002), *Biochemistry* **41**, 3676-3685 (manuscript attached).

[3]. Green DW, Roh H, Pippin JA, Drebin JA. Beta-catenin antisense treatment decreases beta-catenin expression and tumor growth rate in colon carcinoma xenografts (2001) *J. Surg. Res.* **101**, 16-20

[4]. Lopes D, Mayer LD. Pharmacokinetics of Bcl-2 antisense oligonucleotide (G3139) combined with doxorubicin in SCID mice bearing human breast cancer solid tumor xenografts (2002), *Cancer Chemother. Pharmacol.* **49**, 57-68

[5]. Chi KN, Gleave ME, Klasa R, Murray N, Bryce C, Lopes de Menezes DE, D'Aloisio S, Tolcher AW. A phase I dose-finding study of combined treatment with an antisense Bcl-2 oligonucleotide (Genasense) and mitoxantrone in patients with metastatic hormone-refractory prostate cancer (2001), *Clin. Cancer Res.* **7**, 3920-3927

[6]. Bouvet P, Allain FH, Finger LD, Dieckmann T, Feigon J. Recognition of pre-formed and flexible elements of an RNA stem-loop by nucleolin (2001), *J. Mol. Biol.* **309**, 763-75.

[7]. Allain FH, Gilbert DE, Bouvet P, Feigon J. Solution structure of the two N-terminal RNA-binding domains of nucleolin and NMR study of the interaction with its RNA target (2000) *J. Mol. Biol.* **303**, 227-41

Figure 1: Nucleolin Expression on the Surface of Cancer and Normal Cell Lines

A. Surface nucleolin staining.

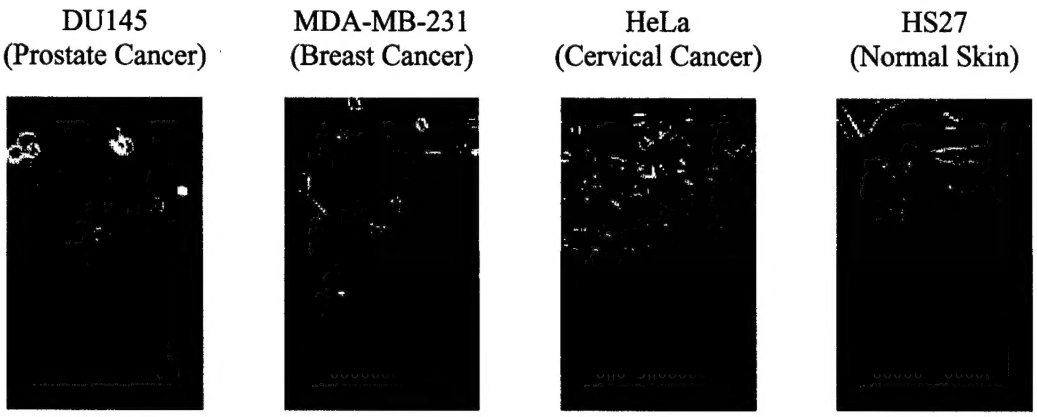

B. Nuclear nucleolin staining.

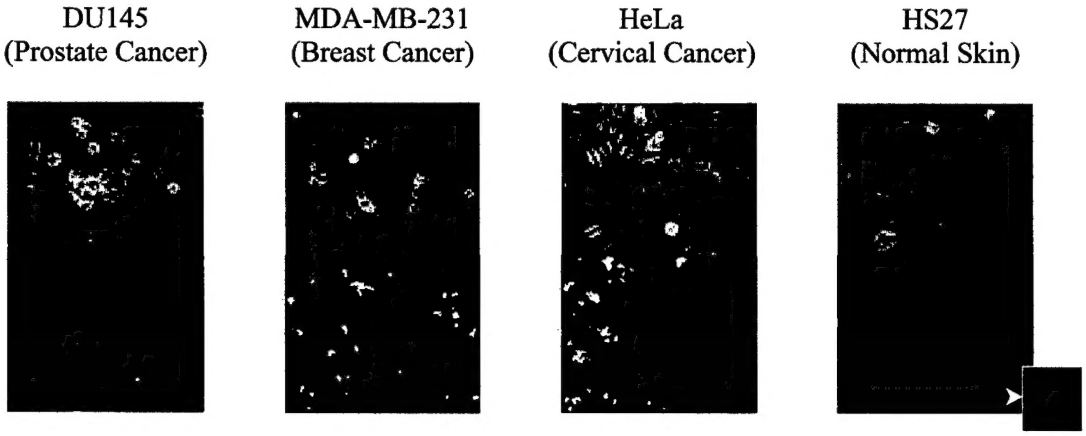

(A) *Phase contrast (upper panel) and immunofluorescent (IF) staining (lower panel) of cell lines using nucleolin antibody without permeabilization of cells to show levels of surface nucleolin (some cytoplasmic staining is also detected). Note that surface staining of non-malignant cells (HS27) is negative, whereas cancer cells are strongly stained.*

(B) *For comparison, phase contrast and IF staining using nucleolin antibody following permeabilization of cells to show levels of nuclear nucleolin. In these preliminary studies, surface/cytoplasmic staining appears to be more tumor-specific than nuclear staining. Magnification shows stained nucleoli in normal HS27 cells.*

Figure 2: Efficient Cellular Uptake of GRO26B is Dependent upon G-quartet Formation and Nucleolin Binding

A.

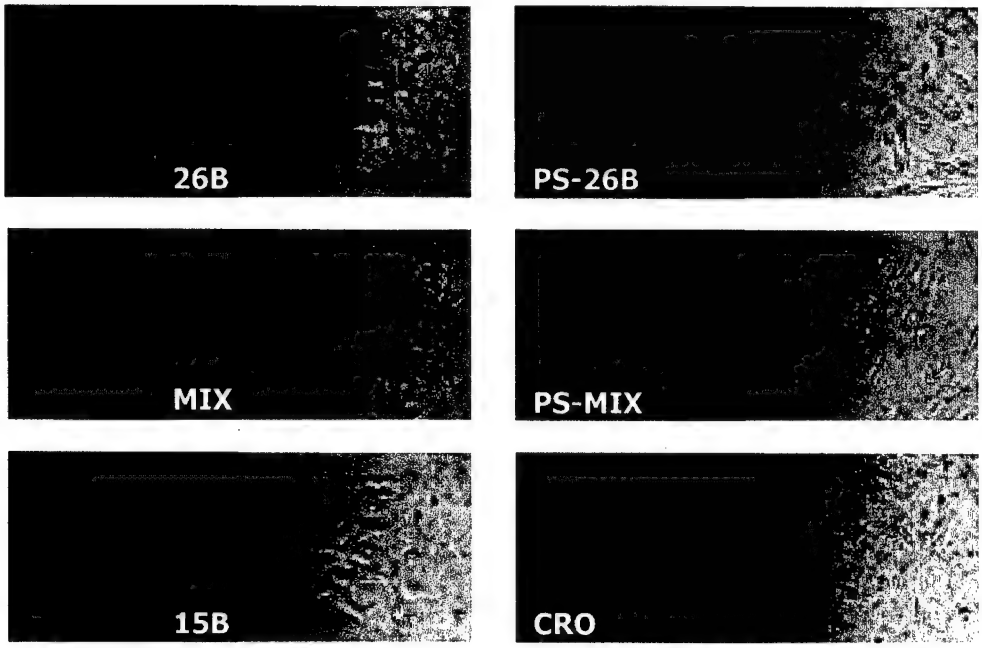

(A) Uptake of FITC-labeled oligonucleotides by DU145 prostate cancer cells. Oligonucleotides (10 μM) were added directly to culture medium and incubated for 24 h. Active GROs with either phosphodiester or phosphorothioate (26B and PS-26B) are taken up more efficiently than control inactive oligonucleotides.

B.

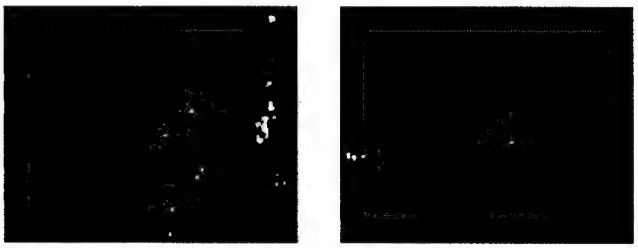

Annealed in KCl *Annealed in NaCl*

(B) Comparison of uptake by DU145 cells FITC-labeled of GRO26B that has been pre-annealed in 10 mM Tris.HCl pH 7.4 containing either 0.1 M NaCl or 0.1 M KCl (which stabilizes G-quartet formation).

Figure 3: Activity of GRO26B in a nude mouse model of human prostate cancer (DU145 xenografts)

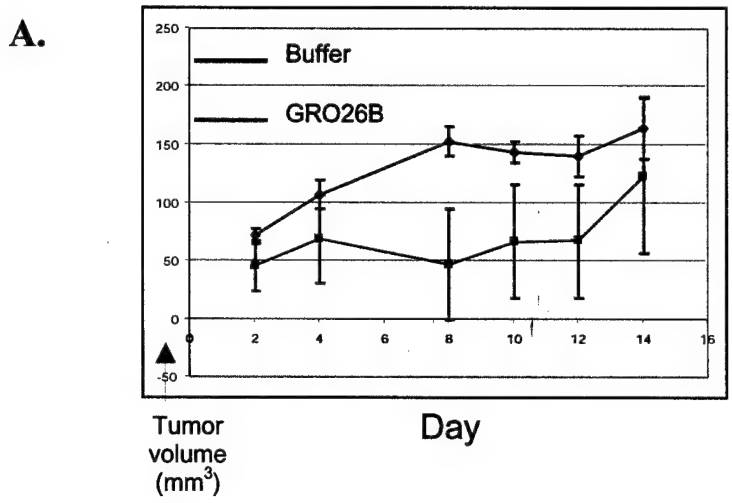

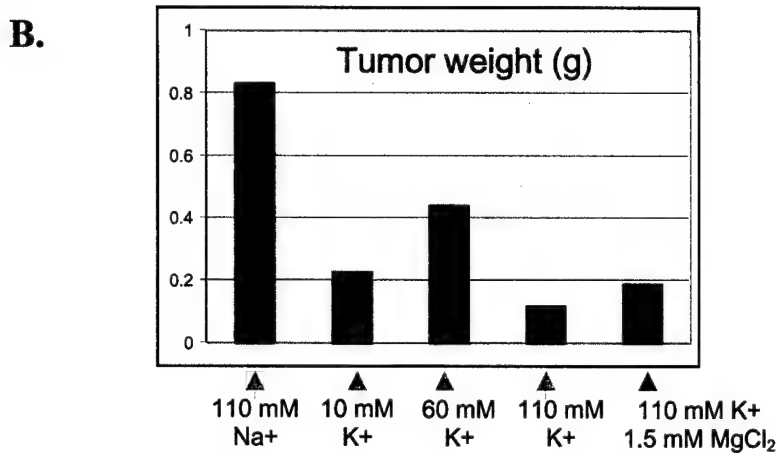

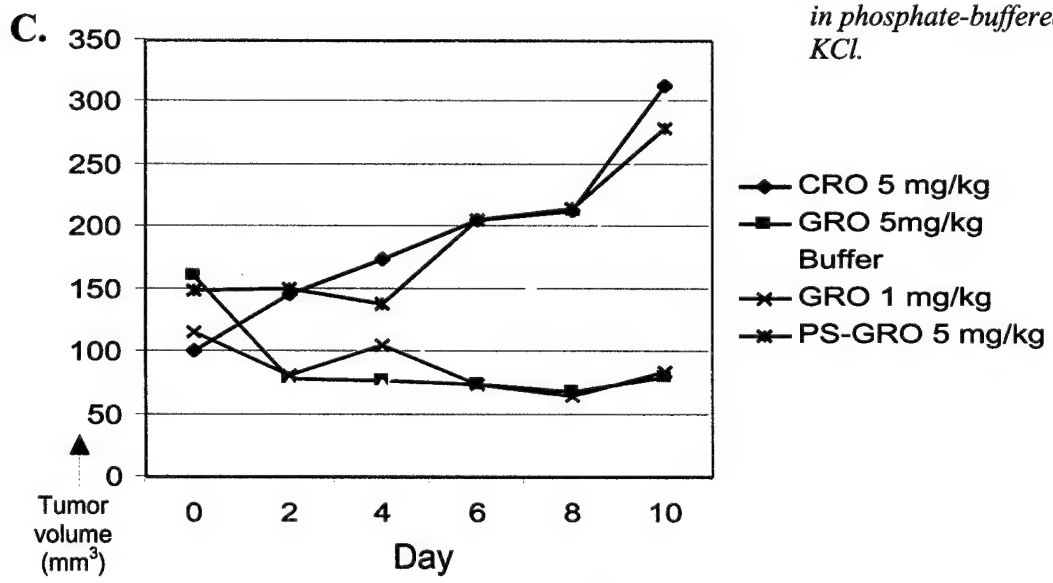

(A) Tumor volume in mice treated by injection (i.p.) of 2 mg/kg GRO26B in PBS or buffer alone (PBS). Treatment began when tumors were palpable (marked as day 0) and mice were injected again on days 2,4,8,10, and 12.

(B) Weight of excised tumors in mice treated as described above, except that GRO26B was pre-annealed in buffers containing 110 mM Na^+ (PBS), or in phosphate buffers containing K^+ at the concentrations shown. Each dose was equivalent to 1.5 mg/kg of GRO26B.

(C) Average tumor volume in mice treated with GRO26B or its phosphorothioate analog or C-rich analog as control. Treatment began when tumors were palpable (marked as day 0). Mice received further injections on days 1, 2, 4, 6, 8. All oligos were pre-annealed in phosphate-buffered 0.1 M KCl.

Drug	Drug → GRO	GRO → Drug
cis-platin	Slight synergy (A)	No effect
taxol	No effect	Additive effect (B)
5-FU	Additive (C)	Synergy (D)
caffeine	Slight synergy (E)	No effect
vinblastine	No effect	No effect
mithramycin	Synergy (F)	Synergy (G)
camptothecin	No effect	Additive (H)

(A) 10 µg/ml cis-platin

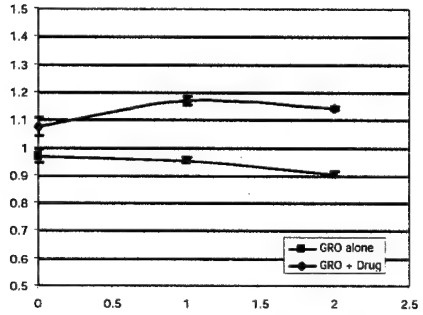

(B) 1.25 nM taxol

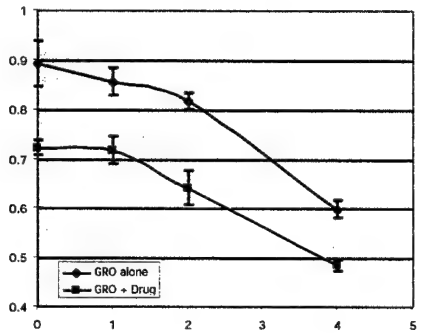

(C) 2 µM 5-FU

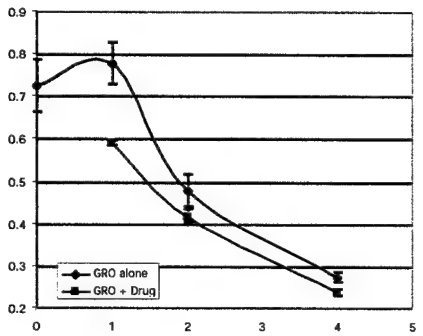

(D) 2 µM 5-FU

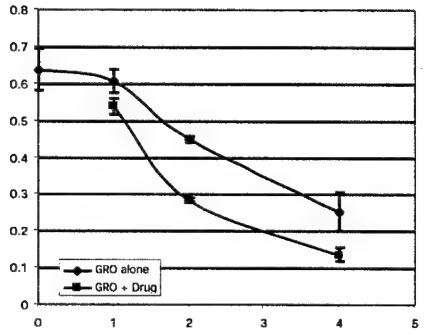

(E) 0.25 mM caffeine

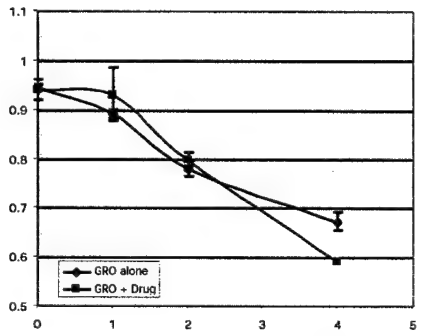

(F) 12.5 nM mithramycin

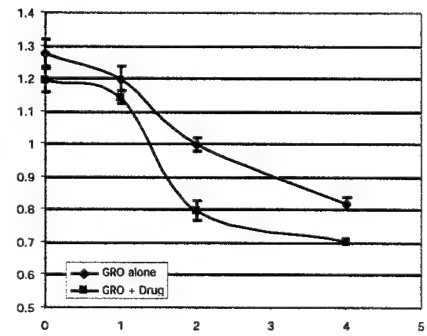

(G) 25 nM mithramycin

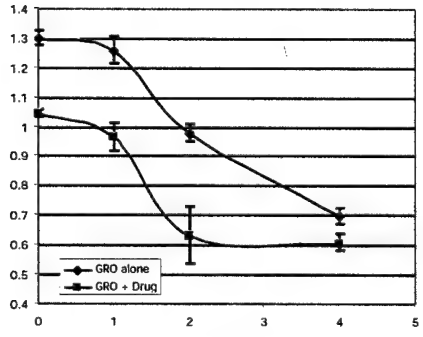

(H) 12.5 nM camptothecin

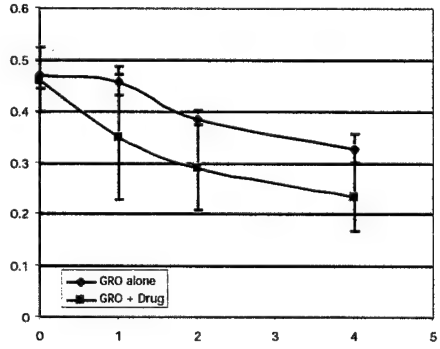

Figure 4: Effect of GRO29A with various chemotherapy and other agents on the proliferation of DU145 prostate cancer cells. Cells were plated in 96 well plates (2,500 cells/well) and incubated for 4 h at 37°C to allow adherence, after which the first agent was added. Cells were incubated for a further 24 h and the second agent was then added. On the sixth day after plating cell viability was assayed by the MTT assay (1). In the graphs, the X-axis is concentration of GRO29A (µM), and the Y-axis is A_{595} (relative cell number).

Antiproliferative Activity of G-Quartet-Forming Oligonucleotides with Backbone and Sugar Modifications†

Virna Đapić,‡,§ Paula J. Bates,§ John O. Trent,§ Alison Rodger,|| Shelia D. Thomas,§ and Donald M. Miller*,§

Department of Biochemistry and Molecular Genetics, University of Alabama at Birmingham, Birmingham, Alabama 35294, James Graham Brown Cancer Center, University of Louisville, Louisville, Kentucky 40202, and Department of Chemistry, University of Warwick, Coventry CV4 7AL, U.K.

Received October 19, 2001; Revised Manuscript Received January 17, 2002

ABSTRACT: Oligonucleotide-based therapies have considerable potential in cancer, viral, and cardiovascular disease therapies. However, it is becoming clear that the biological effects of oligonucleotides are not solely due to the intended sequence-specific interactions with nucleic acids. Oligonucleotides are also capable of interacting with numerous cellular proteins owing to their polyanionic character or specific secondary structure. We have examined the antiproliferative activity, protein binding, and G-quartet formation of a series of guanosine-rich oligonucleotides, which are analogues of GRO29A, a G-quartet forming, growth-inhibitory oligonucleotide, whose effects we have previously described [Bates P. J., Kahlon, J. B., Thomas, S. D., Trent, J. O., and Miller, D. M. (1999) *J. Biol. Chem. 274*, 26369−26377]. The GRO29A analogues include phosphorothioate (PS29A), 2′-*O*-methyl RNA (MR29A), and mixed DNA/2′-*O*-methyl RNA (MRdG29A) oligonucleotides. We demonstrate by UV spectroscopy that all of the modified analogues form stable structures, which are consistent with G-quartet formation. We find that the phosphorothioate and mixed DNA/2′-*O*-methyl analogues are able to significantly inhibit proliferation in a number of tumor cell lines, while the 2′-*O*-methyl RNA has no significant effects. Similar to the original oligonucleotide, GRO29A, the growth inhibitory oligonucleotides were able to compete with the human telomere sequence oligonucleotide for binding to a specific cellular protein. The less active MR29A does not compete significantly for this protein. On the basis of molecular modeling of the oligonucleotide structures, it is likely that the inactivity of MR29A is due to the differences in the groove structure of the quadruplex formed by this oligonucleotide. Interestingly, all GRO29A analogues, including an unmodified DNA phosphodiester oligonucleotide, are remarkably resistant to nuclease degradation in the presence of serum-containing medium, indicating that secondary structure plays an important role in biological stability. The remarkable stability and strong antiproliferative activity of these oligonucleotides confirm their potential as therapeutic agents.

Synthetic oligodeoxynucleotides (ODNs)[1] can inhibit expression of a particular gene and hold considerable interest to researchers as potential therapeutic agents. The strategies by which the ODNs can exhibit such an effect include antisense [ODN binding to a specific mRNA sequence (*1*)] and antigene, also known as the triplex or triple helix approach [ODN binding to a specific DNA sequence (*2*)].

Recent work has shown that ODNs can also exhibit biological effects, which are unrelated to their sequence-specific interactions with nucleic acids (*3*). In particular, guanosine-rich oligonucleotides are emerging as a new class of nonantisense oligonucleotides whose activity can be related to the formation of G-quartet structure. In addition, G-quartet-forming sequences are of interest for other reasons. First, this structural motif likely has biological significance since genomic sequences from telomeric DNA (*4*), immunoglobulin switch region sequences (*5*), the fragile X repeat sequences (*6*), c-myc oncogene (*7*), and the insulin-linked polymorphic region (*8*) can form G-quartets in vitro. Second, there is also considerable interest in the development of molecules that interact with telomeres (which may form G-quartets in vivo) in order to inhibit telomerase (*9*, *10*), an enzyme thought to be a cancer-specific target (*11*−*13*).

Recently, Bates et al. (*14*) reported that a 29-mer, 3′-modified phosphodiester oligonucleotide (GRO29A), exerts a potent growth inhibitory effect against several cancer cell lines in vitro. This oligonucleotide is stabilized by G-quartet formation, and its activity appears to be related to binding to a cellular protein, possibly nucleolin. It is likely that this growth inhibitory activity is caused by GRO29A inhibition of one or more of the normal functions of the protein. Furthermore, it was shown that the GRO29A specifically arrests the cells in the S-phase of the cell cycle. This arrest is characterized by inhibition of the DNA synthesis (*15*).

† This work was supported by NCI Grants RO1CA42664 and RO1CA54380 and U.S. Army Prostate Research Initiative PC970218.

* To whom correspondence should be addressed. Phone: (502) 562-4369. Fax: (502) 562-4368. E-mail: donaldmi@ulh.org.

‡ University of Alabama at Birmingham.

§ University of Louisville.

|| University of Warwick.

[1] Abbreviations: ODN, oligodeoxynucleotides; GRO, G-rich oligonucleotide; PBS, phosphate-buffered saline; DMEM, Dulbecco's modified Eagle medium; FCS, fetal calf serum; MTT, 3-(4,5-dimethylthiazol-2-yl)-2,5-diphenyltetrazolium bromide; CD, circular dichroism; PBC, periodic boundary conditions; PME, particle mesh Ewald summation; HIV, human immunodeficiency virus.

10.1021/bi0119520 CCC: $22.00
Published on Web 02/20/2002

Table 1: Synthetic Oligonucleotides

oligo-nucleotide	sequence	properties
GRO29A	5′-TTT GGT GGT GGT GGT TGT GGT GGT GGT GG-3′	phosphodiester backbone; 3′-aminoalkyl group modification; deoxyguanosines and deoxythymidines; original antiproliferative oligonucleotide
PS29A	5′-*TTT GGT GGT GGT GGT TGT GGT GGT GGT GG*-3′	phosphorothioate backbone; deoxyguanonsies and deoxythymidines; analogue of GRO29A
MRdG29A	5′-UUU GGU GGU GGU GGU UGU GGU GGU GGU GG-3′	2′-*O*-methyluracil and deoxyguanosines (RNA); chimeric analogue of GRO29A
MR29A	5′-**UUU GGU GGU GGU GGU UGU GGU GGU GGU GG**-3′	2′-*O*-methyluracil and 2′-*O*-methylguanosines (RNA); analogue of GRO29A
29A-OH	5′-TTT GGT GGT GGT GGT TGT GGT GGT GGT GG-3′	phosphodiester backbone; no 3′ modifications; deoxyguanosines and deoxythymidines; analogue of GRO29A
TEL	5′-TTA GGG TTA GGG TTA GGG TTA GGG-3′	phosphodiester backbone; human telomere sequence
CH1	5′-UUU GGU GGU GGU GGU UGU GGU GGU GGU GG-3′	chimeric 2′-*O*-methyluracil and deoxyguanosine (RNA); **G** at position 17 was replaced with 2′-*O*-methyl G in studies determining the importance of the loop region
CH2	5′-**UUU GGU GGU GGU GGU U*G*U GGU GGU GGU GG**-3′	chimeric 2′-*O*-methyluracil and 2′-*O*-methylguanosine (RNA); *G* at position 17 was replaced with deoxyguanosine in studies determining the importance of the loop region
15B	5′-TTG GGG GGG GTG GGT-3′	phosphodiester backbone; 3′-aminoalkyl group modification; deoxyguanosines and deoxythymidines; control G-rich oligonucleotide with negligible antiproliferative activity
PS15B	5′-*TTG GGG GGG GTG GGT*-3′	phosphorothioate backbone; deoxyguanosines and deoxythymidines; analogue of 15B
MR15B	5′-**UUG GGG GGG GUG GGU**-3′	2′-*O*-methyluracil and 2′-*O*-methylguanosines (RNA); analogue of 15B
P2C	5′-TCT AGA AAA ACT CTC CTC TCC TTC CTC CCT CTC CA-3′	unmodified phosphodiester oligonucleotide; control mixed sequence

Because phosphodiester oligonucleotides are extremely sensitive to nuclease degradation in biological media, they are usually considered unsuitable for experiments in vivo and in cell culture systems. Most antisense studies have therefore been carried out using modified oligonucleotides, including phosphorothioate derivatives (*16*, *17*). Despite their increased stability, toxicities have been observed in animal studies. The major toxicities are thought to be due to the polyanionic nature of these oligonucleotides, which allows them to bind to numerous cellular proteins. In addition, they appear to be immunostimulatory, inducing the expression of cytokines and chemokines (*17*−*19*). However, despite their limitations, there have been numerous studies reporting sequence-specific effects of phosphorothioate oligonucleotides, and these have resulted in several clinical trials (*20*−*23*). These studies have shown that oligonucleotides can be safely administered to humans.

To fully characterize the antiproliferative activity of G-rich oligonucleotides such as GRO29A, we have examined several analogues with modified sugar−phosphate backbones. Here we present the results of our evaluation of the antiproliferative activity, protein binding, G-quartet formation, and stability in serum-containing medium of these analogues. We have demonstrated that phosphorothioate and mixed DNA/2′-*O*-methyl analogues of GRO29A exhibit strong antiproliferative activity, which is attributed to their ability to bind to the cellular protein, nucleolin, as well as their ability to form stable G-quartet structures. The formation of G-quartets renders these oligonucleotides extremely stable against nuclease degradation, and this stability is maintained without additional modifications. This is the first reported example, to the authors' knowledge, of 2′-*O*-methyl RNA and mixed 2′-*O*-methyl RNA:DNA forming G-quartet-containing structures.

EXPERIMENTAL PROCEDURES

Oligonucleotides. All oligonucleotides were purchased from Oligos Etc. (Wilsonville, OR). The integrity of the oligonucleotides was verified by 5′-radiolabeling followed by analysis on denaturing polyacrylamide gels. Oligonucleotides were resuspended in phosphate-buffered saline (PBS) at a concentration of 500 μM and annealed by boiling for 5 min and cooling slowly to room temperature.

Detection of G-Quartets by UV Spectroscopy. Oligonucleotides were resuspended in Tm buffer (140 mM KCl, 2.5 mM $MgCl_2$, and 20 mM Tris·HCl, pH 8.0) at a final concentration of 2 μM. Oligonucleotides were annealed by the method described above and were further incubated at 4 °C overnight. Thermal denaturation−renaturation experiments were carried out using an Ultrospec 2000 instrument equipped with a Peltier effect heated cuvette holder and temperature controller (Amersham Pharmacia Biotech). A temperature range of 25−95 °C was used to monitor absorbance at 295 nm at a heating/cooling rate of 0.5 °C/min.

Circular Dichroism Study. Oligonucleotides, at a final concentration of 5 μM or 2.5 μM, were resuspended in 10 mM sodium phosphate buffer, pH 7.0, containing 0.1 M KCl (final volume, 1 mL), were boiled for 5 min, and annealed at 60 °C for 56 h. Samples were analyzed on a Jasco J-175 spectropolarimeter. Spectra were collected over 16 scans at 100 nm/min, 1 s response time, and 1 nm bandwidth. Cuvettes, 4 mm wide, with black quartz sides to mask the light beam were used for the measurements.

Cell Growth Assay. Cells were plated at a density of 10^3 cells/well in a 96-well plate in Dulbecco's modified Eagle medium (DMEM) supplemented with 10% fetal calf serum (FCS), which has been heat inactivated for 30 min at 55 °C. After 4 h to allow adherence of cells, oligonucleotides were

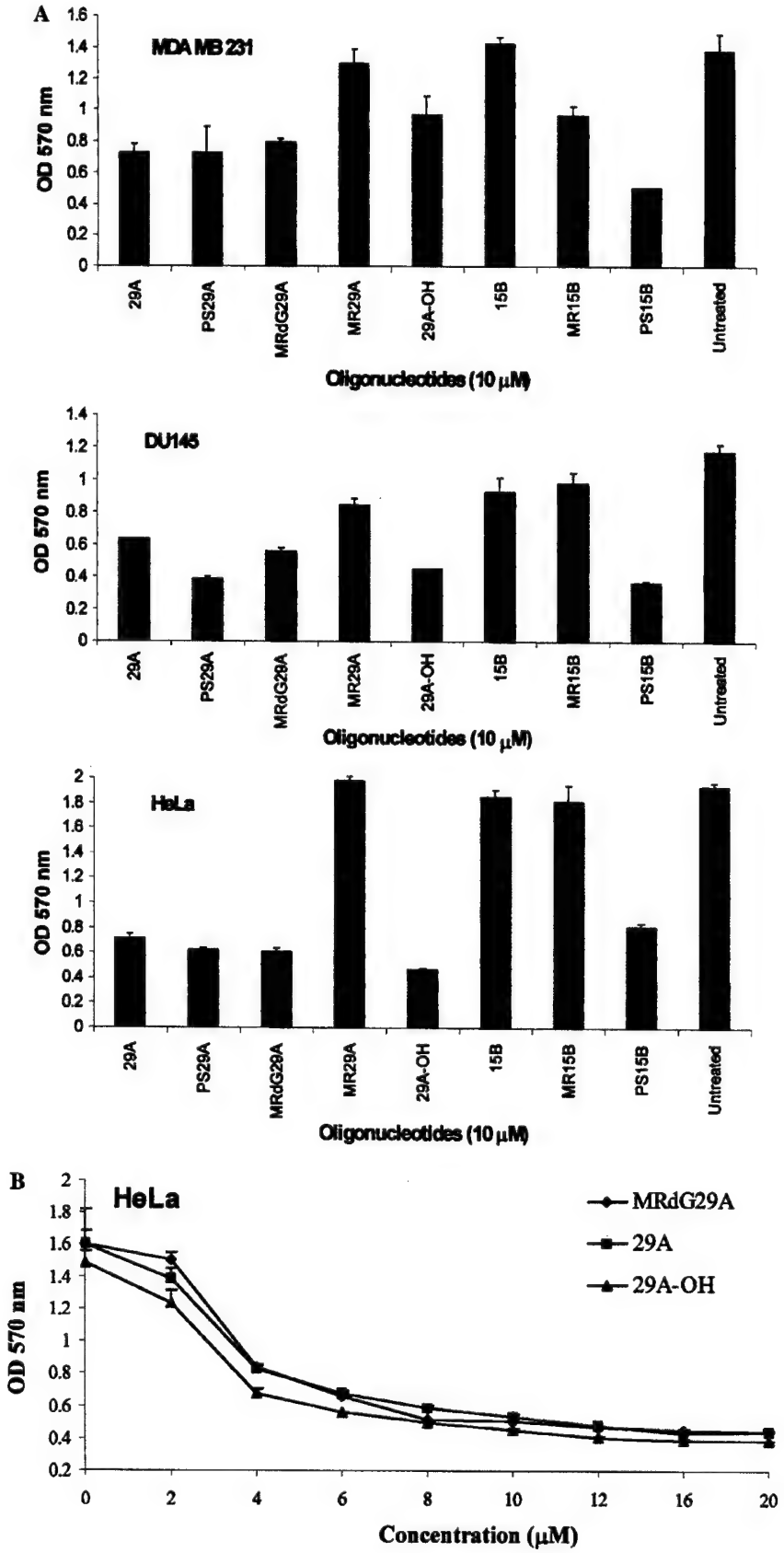

FIGURE 1: Activity of G-rich oligonucleotides in cancer cell lines determined with MTT assay. (A) Cancer cell lines were treated with G-rich oligonucleotides by direct addition of the GRO to the culture medium. The cell type used is shown in the upper left corner of each graph. (B) Dose−response curve for HeLa cells treated with G-rich oligonucleotides. Symbols representing oligonucleotides are shown in the upper right corner of the graph. Experiments for both figures were performed in triplicate, and bars represent the standard error of the data.

added directly to the culture medium to give a final concentration of 10 μM. Cells were further incubated at 37 °C in 10% CO_2. Seven days after the addition of oligonucleotides, cell viability was assayed using the MTT assay (*24*). Culture medium was not replaced during the 7 days. The experiments were performed in triplicate, and bars represent the standard error of the data.

Electrophoretic Mobility Shift Assay (EMSA). TEL oligonucleotide was labeled with ^{32}P using T4 kinase. Labeled oligonucleotide (2×10^4 cpm per reaction, final concentration approximately 1 nM) was preincubated alone or in the presence of an unlabeled competitor oligonucleotide for 30 min at 37 °C. HeLa nuclear extracts (bandshift grade; Promega, Inc., Madison, WI) were added, and samples were incubated for an additional 30 min at 37 °C. Preincubation and binding reactions were carried out in buffer A (20 mM Tris·HCl, pH 7.4, 140 mM KCl, 1 mM dithiothreitol, 0.2 mM phenylmethanesulfonyl fluoride, and 8% v/v glycerol). Electrophoresis was carried out using 5% polyacrylamide gels in TBE buffer (90 mM Tris−borate and 2 mM EDTA).

Stability of Oligonucleotides in Cell Culture Medium. Labeled oligonucleotides (total of 10^6 cpm of each) were incubated in the cell culture medium (DMEM supplemented with 10% FCS, heat inactivated at 55 °C for 30 min) at 37 °C for 0, 4, 48, 72, and 120 h. At each time point, 10 μL of sample was removed, briefly centrifuged, and quick-frozen by placement in a dry ice/ethanol mixture. Samples were stored at −80 °C until analysis. Prior to analysis, samples were quickly thawed out at 37 °C, and 10 μL of loading buffer (98% deionized formamide, 10 mM EDTA, pH 8.0, 0.025% bromophenol blue, and 0.025% xylene cyanol FF) was added to each sample. Samples were boiled for 5 min and placed on ice prior to being analyzed by denaturing polyacrylamide gel electrophoresis on a 7 M urea/16% polyacrylamide gel.

Stability of Oligonucleotides in Cytoplasmic Extracts. Labeled oligonucleotides (5×10^5 cpm of each) were incubated in HeLa S-100 [prepared as previously described (*25*)], 2 μg total protein, at 37 °C for up to 8 h. At each time point, 10 μL of sample was removed and quick-frozen as above. Samples were analyzed in the same way as for the culture medium stability experiments.

Molecular Modeling of GRO29A and Its Analogues MR29A and MRdG29A. The dimeric chair model of the antiparallel GRO29A structure was generated using the human telomere solution structure (*26*). This final model generated by the protocol below was modified to produce the starting model of the analogous structures, which consequently were examined using the same protocol. The structure was minimized by steepest descents (1000 steps) and Polack−Riberie (2000 steps) conjugated gradient methods. The AMBER* force field and the GB/SA implicit water continuum solvation within Macromodel 7.0 (*27*) were used for all minimization and molecular dynamics calculations. The minimized structure was equilibrated at 300 K for 100 ps (1.5 fs time step) using molecular dynamics. The final structure was generated by averaging a further molecular dynamics production phase of 1 ns, sampling at 1 ps in the last 50 ps, with subsequent minimization. Fully solvated molecular dynamics calculations using AMBER 6.0 with PBC and PME are ongoing and will be reported separately. The molecular surfaces for Figure 5A were generated in INSIGHTII (*28*). Analysis of the grooves of GRO29A, MR29A, and MRdG29A was done using GrooveView (*29*). This program generates the molecular surfaces of the region of interest and provides cross-section slices (1.6 Å apart) of the surface perpendicular to the groove axis (Figure 5B).

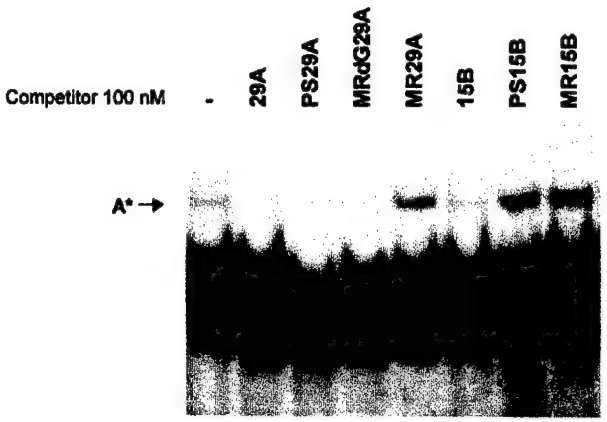

FIGURE 2: Electrophoretic mobility shift assay with 5′-labeled TEL oligonucleotide. Radiolabeled TEL was incubated with nuclear protein extract alone or in the presence of unlabeled, competitor G-rich oligonucleotides and control. Oligonucleotide samples were incubated in buffer A (20 mM Tris·HCl, pH 7.4, 140 mM KCl, 1 mM dithiothreitol, 0.2 mM phenylmethanesulfonyl fluoride, and 8% v/v glycerol) and electrophoresed on 5% polyacrylamide gels in TBE buffer. Band A* represents a complex formed between the TEL and the protein(s), which is competed specifically by active GROs.

RESULTS

Modified G-Rich Oligonucleotides Inhibit Cancer Cell Proliferation in Cell Culture. The oligonucleotides were tested for antiproliferative activity in three cancer cell lines, derived from cervical (HeLa), breast (MDA-MB 231), and prostate (DU 145) carcinomas. The structure and modifications of all oligonucleotides are described in Table 1. These oligonucleotides included a phosphorothioate analogue, a full 2′-*O*-methyl RNA analogue, and an analogue with deoxyguanosines and 2′-*O*-methyluridines. The original GRO29A was the only one with 3′ amino group modification. We also tested 29A-OH, a phosphodiester analogue without the 3′-propylamino group, to determine whether 3′ modification was necessary for oligonucleotide stability. Control oligonucleotides were analogues of GRO15B, which was previously found to have very weak antiproliferative activity (*14*).

Figure 1A demonstrates the growth inhibitory activity of the various oligonucleotides as measured by the MTT assay, which determines the relative number of viable cells. In each of the cell lines tested, we observed that the GRO29A analogues PS29A, MRdG29A, and 29A-OH had similar or greater growth inhibitory activity compared to GRO29A. The analogue containing all 2′-*O*-methyl RNA nucleotides, MR29A, was inactive or had only weak antiproliferative activity. Of the control oligonucleotides, GRO15B had a much weaker antiproliferative effect, as expected, and the 2′-*O*-methyl RNA (MR15B) control had a similar effect. However, the phosphorothioate control (PS15B) had significant antiproliferative effect that equaled or exceeded that of PS29A. Possible explanations for this observation will be discussed below.

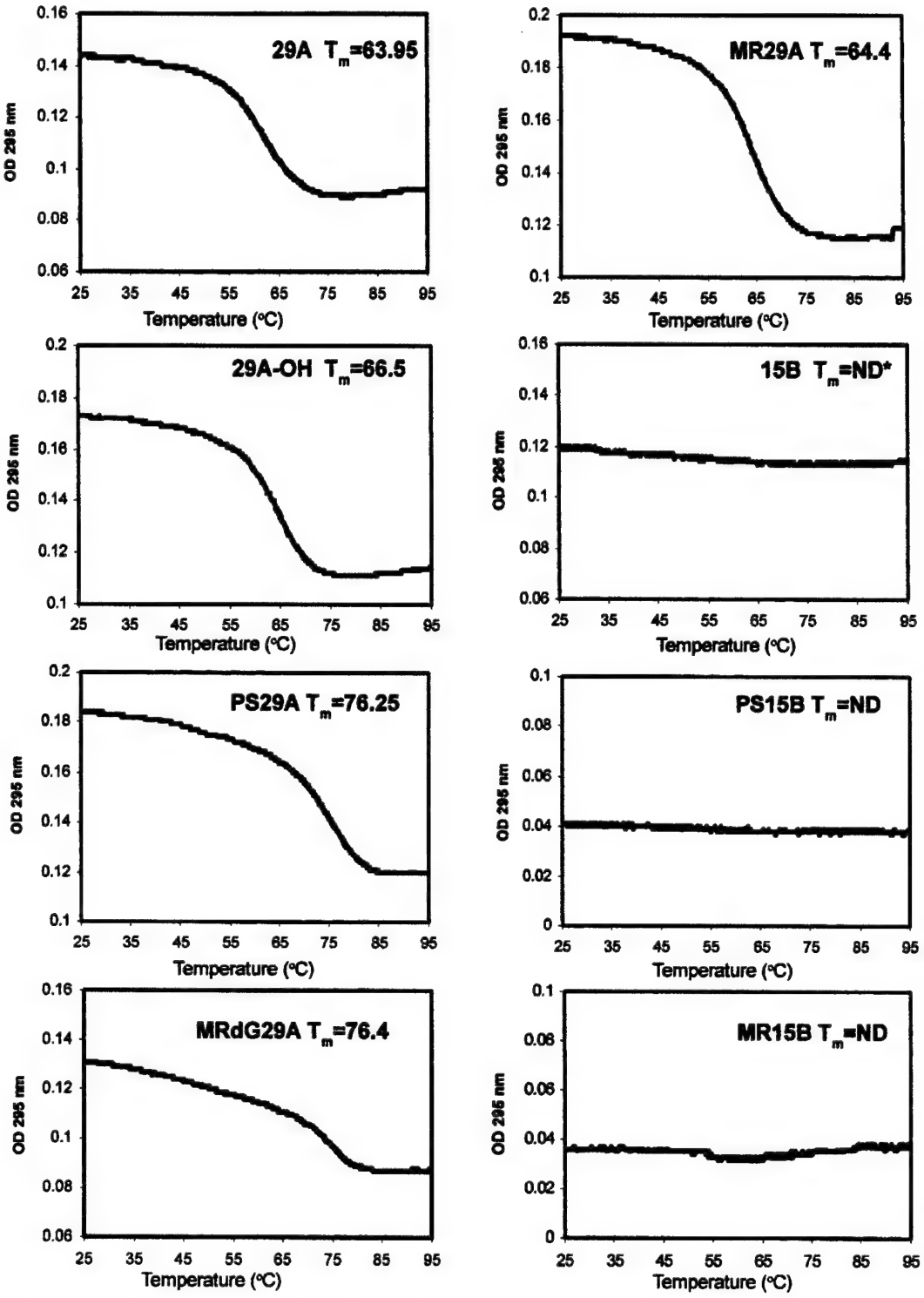

FIGURE 3: G-quartet formation of G-rich oligonucleotides assessed by UV thermal renaturation studies. The oligonucleotide name is shown in the upper right corner of each graph. Experiments were carried out in Tm buffer (20 mM Tris·HCl, pH 8.0, 140 mM KCl, and 2.5 mM $MgCl_2$). ND = not detected.

We also determined the GI_{50} (50% growth inhibition) for the active oligonucleotides. In HeLa cells treated with a single dose of oligonucleotide and assayed after 7 days, the GI_{50} values were similar for GRO29A, MRdG29A, and PS29A (4 μM; see Figure 1B).

Relationship between Growth Inhibitory Activity and Protein Binding. It was previously reported (*14*) that the antiproliferative activity of G-rich oligonucleotides correlated with their ability to bind to a specific cellular protein, which also binds to the human telomere sequence oligonucleotide. To test whether the antiproliferative activity of the GRO29A analogues is also related to binding to this protein, we used a competitive electrophoretic mobility shift assay (EMSA). 5′-Radiolabeled TEL oligonucleotide (a G-quartet-forming oligonucleotide) representing the human telomere sequence was incubated with HeLa nuclear extracts alone or in the

presence of unlabeled competitor oligonucleotide, and the interaction was examined by an EMSA. Figure 2 depicts the formation of the TEL−protein complex and the ability of the unlabeled oligonucleotides to compete for binding to the protein(s). The experiment shows that the GRO29A analogues with antiproliferative activity (PS29A and MRdG29A) were able to compete with TEL for binding with the protein, whereas the inactive analogue, MR29A, was not able to compete for binding. This is indicated by the reduced intensity of band A when active analogues were included. Of the control oligonucleotide analogues, none were able to compete significantly for protein binding. This indicates that the protein is specifically recognizing some characteristic of active GRO29A analogues, rather than simply binding to G-rich oligonucleotides. The obvious exception to the observed correlation between biological activity and binding to the specific protein is PS15B, which has high antiproliferative activity but does not compete for protein binding. We conclude from this that this oligonucleotide is exerting its effect via a mechanism that is different from that of GRO29A and its active analogues. This is unsurprising in light of what is known of the nonspecific effects of phosphorothioate oligonucleotides, which have a much higher level of nonspecific protein binding compared to phosphodiester oligonucleotides (*17*, *19*). Because the PS analogue of GRO29A is able to compete for protein binding, it seems likely that the activity of PS29A stems from a combination of both nonspecific effects and specific GRO29A-like effects.

Modified G-Rich Oligonucleotides Form G-Quartets. The failure of MR29A, the 2′-*O*-methyl oligonucleotide, to inhibit the growth of cells may be a result of a number of factors. One explanation would be that the 2′-*O*-methyl RNA could not form G-quartet structures. Alternatively, it may form a G-quartet structure, which is significantly different from that of GRO29A, and therefore would not be a substrate for binding to the active GRO-specific protein.

To investigate the possibility that the 2′-*O*-methyl RNA analogue cannot form G-quartets, we have analyzed G-quartet formation of all GRO29A analogues. A UV thermal denaturation−renaturation method described by Mergny et al. (*30*) was employed for this study. This method is based on the fact that dissociation of antiparallel G-quartets (those formed in folded dimeric or monomeric molecules) leads to decreased absorbance at 295 nm. Figure 3 shows the annealing curves for the oligonucleotides tested. G-quartet formation is indicated with a clear transition, as seen for GRO29A, which has a melting temperature of approximately 63 °C. MRdG29A, MR29A, and PS29A all showed a similar profile to the one observed for GRO29A, with similar or slightly higher T_m. This profile was reversible, with a small hysteresis (2−3 °C difference between heating and cooling curves). None of the control GRO15B analogues exhibited transitions consistent with G-quartet formation, even though they contain contiguous runs of guanosines. We also tested the melting of this oligonucleotide by monitoring the absorbance at 260 nm, which would indicate parallel tetrameric quadruplet formation, but that also did not show the presence of G-quartet structure.

Circular Dichroism Evaluation of G-Quartets. The method used to detect T_m for the oligonucleotides has been shown to be specific for antiparallel G-quartets. We further wanted to test the folding of GRO29A and its analogues by

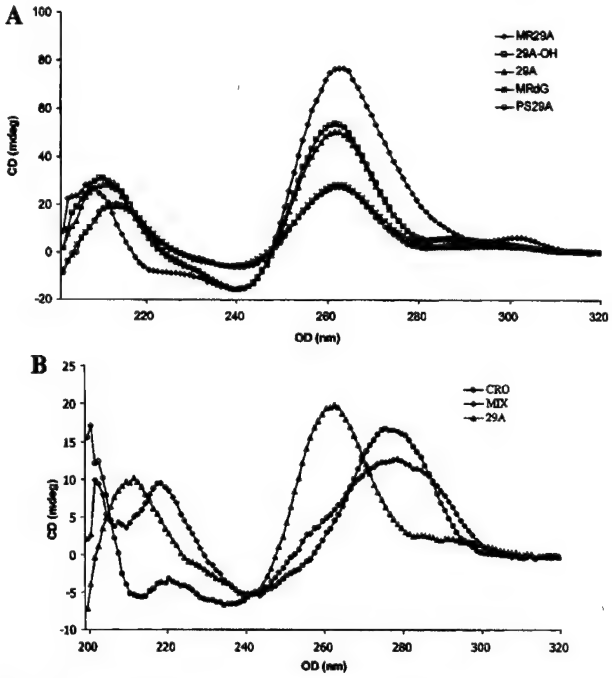

FIGURE 4: (A) CD spectra of MR29A, 29A-OH, 29A, MRdG, and PS29A. CD data were obtained with a 5 μM strand concentration in the presence of 0.1 M KCl at 25 °C. (B) CD spectra of CRO, mix, and 29A oligonucleotides (2.5 μM strand concentrations).

employing circular dichroism (CD) measurements. It is generally thought that parallel-type G-quartets, when analyzed by CD, have a positive ellipticity maximum at 264 nm and a negative ellipticity minimum at 240 nm, while the antiparallel G-quartet structures have a strong positive maximum between 290 and 295 nm and a minimum at 265 nm (*31*). However, we have found (Bates and Rodger, unpublished data) that some G-quartets known to form in the antiparallel orientation exhibit the classical parallel G-quartet spectra with a positive 264 nm peak. Jing et al. reported a similar finding (*32*), where analysis of a potent anti-HIV oligonucleotide T30177 showed CD spectra consistent with parallel G-quartets. However, this oligonucleotide forms antiparallel G-quartets.

G-rich oligonucleotide 29A appears to fall into this category. The CD spectrum (Figure 4A) shows that 29A exhibits a strong 264 nm peak characteristic of G-quartets. This signature peak is absent in mixed sequence or C-rich oligonucleotides (Figure 4B). Figure 4A further shows that all of the GRO29A modified analogues have negative ellipticity minimum at 240 nm and a positive ellipticity maximum at 264 nm. MR29A has a slight shift with an additional minor peak between 300 and 310 nm. The difference is most likely due to the 2′-*O*-methyl groups contributing to the different stacking of G-quartets.

Molecular Modeling of GRO29A Analogues. To investigate whether the structure of the G-quartet species formed by inactive MR29A was different from that formed by GRO29A and MRdG29A, we carried out molecular modeling studies. The molecular dynamics simulations produced stable models for GRO29A, MR29A, and MRdG29A, which are consistent with all experimental data (Figure 5A). The models were similar with respect to G-quartet stability and overall structure but had major differences in their topological features. The cross sections of the solvent-accessible surface

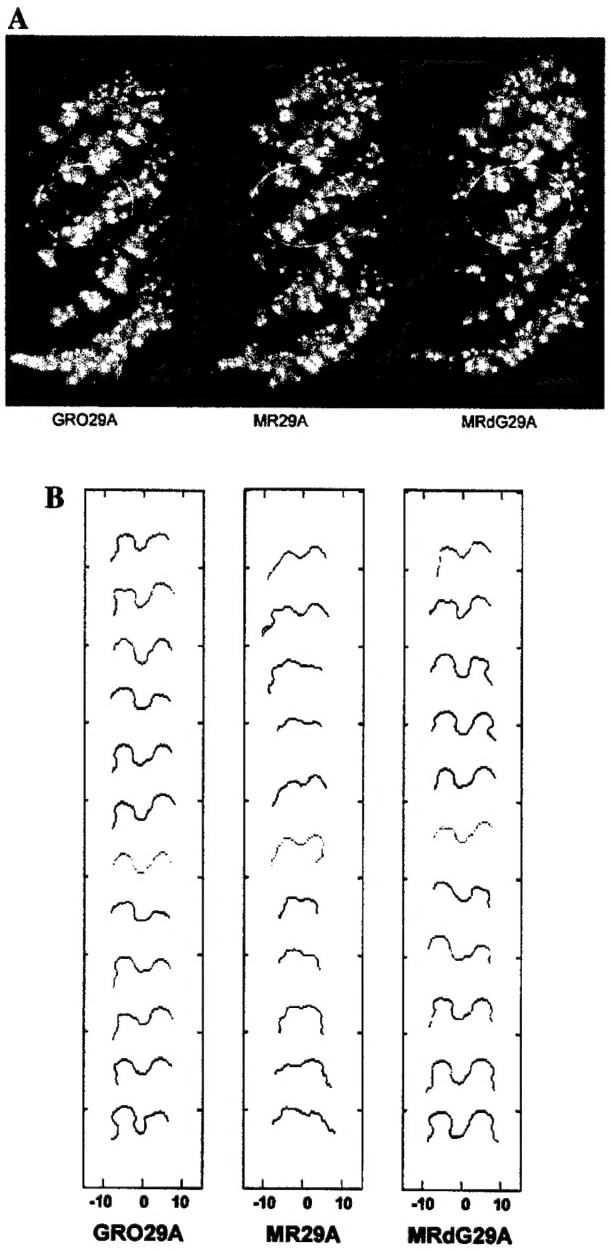

FIGURE 5: Structural studies of G-rich oligonucleotides. (A) Molecular surface representations of the molecular models of GRO29A, MR29A, and MRdG29A. (B) Cross sections of the solvent-accessible surface of the circled regions of (A) generated by GrooveView (*29*).

of the circled regions in Figure 5A are shown in Figure 5B. The quadruplex grooves of GRO29A and MRdG29A had similar characteristics, whereas in the case of MR29A, the depth and shape of the grooves were considerably altered by the effect of the 2′-*O*-methyl sugar substituents of the guanosines. The effect of the 2′-*O*-methyl groups in MR29A is to change the nature of the grooves, thus making the four grooves significantly different. This is typified by the fact that the region of the curve chosen for the analysis does not have the 2′-*O*-methyl groups located in that groove, so the narrowing of the groove is not simply due to "filling" the groove with the substituents. The average depth of this groove region for GRO29A and MRdG29A is approximately 5 Å whereas the groove in MR29A ranges from 0 to 2 Å.

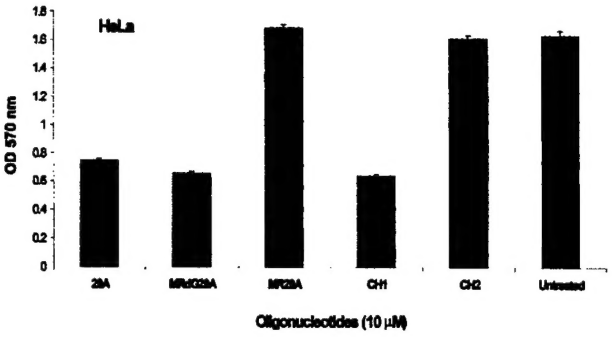

FIGURE 6: Loop region studies. Loop region studies were carried out with chimeric G-rich oligonucleotides. Base substitutions are indicated in Table 1. Activity was assayed using the MTT assay. Experiments were performed in triplicate, and bars represent the standard error of the data.

Table 2: Guanosines in the Quartet Core and Loop Regions

oligonucleotide	quartet core	loop	activity
GRO29A	deoxyguanosines	deoxyguanosines	++++
MRdG29A	deoxyguanosines	2′-*O*-methyl RNA	++++
MR29A	2′-*O*-methyl RNA	2′-*O*-methyl RNA	−
CH1	deoxyguanosines	2′-*O*-methyl RNA	++++
CH2	2′-*O*-methyl RNA	deoxyguanosines	−

Study of the Loop and G-Quartet Region of MR29A and MRdG29A. To exclude the possibility that the activity of MRdG29A was a result of differences in the loop rather than G-quartet structure, we designed two chimeric oligonucleotides, CH1 and CH2, where CH1 had deoxyguanosines in the G-quartet region and 2′-*O*-methylguanosines in the loop region. Both chimeric oligonucleotides were tested in cell growth assay (MTT) using the HeLa cell line to determine their antiproliferative activity following the substitutions (Figure 6). The activity of CH1 was not diminished due to the change in sequence, while CH2, which had 2′-*O*-methylguanosines in the G-quartet core and deoxyguanosines in the loop region, had no antiproliferative activity (see Table 2). This allowed us to conclude that the loop is unlikely to play a direct role in the activity.

Stability of G-Rich Oligonucleotides in Serum-Containing Medium and Cellular Extracts. The poor stability of unmodified oligonucleotides in vivo presents one of the major obstacles in their development as potential therapeutic drugs. Therefore, we investigated the stability of unmodified and modified oligonucleotides in serum-containing medium as well as in cellular extracts.

Figure 7A shows that all of the G-quartet-forming oligonucleotides were stable in serum-containing medium for at least 72 h. We also tested 29A-OH, a phosphodiester analogue of GRO29A without the 3′ modification, and compared it to a random oligonucleotide P2C, which has no detectable secondary structure. The G-quartet forming oligonucleotide, 29A-OH, was stable for over 5 days while the P2C oligonucleotide was degraded within 1 h of being added to the serum-containing medium (Figure 7B). Similar indications of stability were obtained when oligonucleotides were tested in S-100 extracts of HeLa cells (not shown). All G-quartet-forming oligonucleotides were completely undegraded after 8 h at 37 °C in the presence of 2 μg of protein extract.

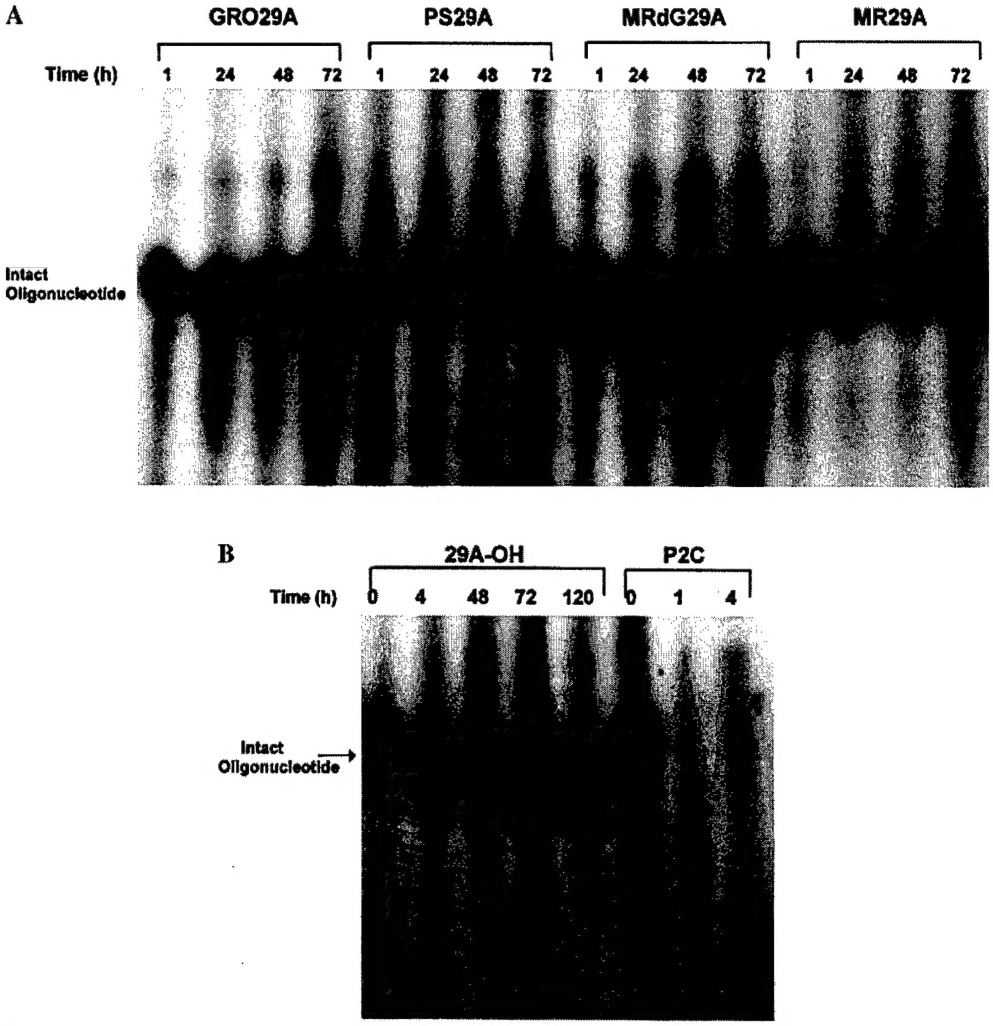

FIGURE 7: Stability of G-rich oligonucleotides in serum-containing medium. (A) 5′-Labeled oligonucleotides were incubated for the times indicated in the presence of culture growth medium (DMEM supplemented with 10% FCS, heat inactivated at 55 °C for 30 min). Samples were analyzed on a denaturing (7 M urea) 16% polyacrylamide gel. (B) 5′-Labeled G-rich oligonucleotide 29A-OH and an unmodified, phosphodiester oligonucleotide, P2C, were incubated for the times indicated in the presence of culture growth medium.

It is most remarkable that 29A-OH, an unmodified phosphodiester oligonucleotide, is stable for over 5 days in serum-containing medium. Since phosphodiester oligonucleotides (e.g., P2C) are generally degraded within minutes under such conditions, it appears that G-quartet formation is extremely important for oligonucleotide stability. Presumably, the folded structure of 29A-OH prevents access by nucleases. It is also possible that the novel structure formed by these oligonucleotides is unrecognized by any helicases, which may unravel them. The high stability of GRO29A and its analogues also suggests that the intact oligonucleotide, rather than a degradation product, is the active species.

In fact, the potential therapeutic success of any oligonucleotide therapy will depend on the ability of the oligonucleotide to remain intact under in vivo conditions. Our results suggest that any of the GRO29A analogues tested would have sufficient stability in vivo to make them therapeutically useful.

Another G-quartet-forming oligonucleotide with a phosphodiester backbone (except for two terminal phosphorothioate linkages) has also been reported to have a high biological stability due to its tertiary structure (*33*) and is currently being tested as an anti-HIV agent (*34*).

DISCUSSION

We have studied the protein binding characteristics and cell growth inhibitory effects of G-rich oligonucleotides that are backbone-modified analogues of the antiproliferative oligonucleotide, GRO29A. Previous work has identified the protein binding ability of GRO29A (*14*), and more recently, it was shown that this oligonucleotide can arrest the cells in the S-phase and inhibit DNA replication (*15*). The results of the present studies show that some, but not all, of the modified analogue oligonucleotides have strong antiproliferative effects against several cancer cell types. It is likely that these effects are not due to any antisense or antigene activity but rather are related to their specific secondary structure and its recognition by cellular proteins.

Previous reports have indicated that the nonantisense effects of G-rich oligonucleotides are related to their secondary structure (G-quartets) and protein binding (*35*, *36*). By employing UV and CD spectroscopy, we have detected a characteristic melting curve, indicating G-quartet formation by all modified GRO29A analogues tested. To our knowledge, this is the first report of full 2′-*O*-methyl RNA and mixed 2′-*O*-methyl RNA:DNA sequences being able to form

G-quartets. Interestingly, a recent paper showed that mRNA sequences involved in synaptic function or dendritic growth are capable of forming G-quartets. Moreover, these sequences were specifically targeted by the FMRP, a protein absent in the fragile X syndrome (*37*). This suggests a possible in vivo role for G-quartet formation by RNA sequences.

However, the presence of G-quartet formation was not sufficient for antiproliferative activity, since MR29A, which forms G-quartets, had no significant activity. Significant growth inhibitory activity was only observed for those G-quartet-forming oligonucleotides that could also compete for binding to a specific cellular protein(s) in a mobility shift assay. This supports our hypothesis that antiproliferative activity is mediated by binding to the protein.

Sequences containing G-quartets have been shown to bind to numerous cellular proteins (*5*, *14*, *38*–*40*). This relationship could be a part of transcriptional regulation, a general regulation of gene expression, telomere maintenance, and cell growth regulation. The proposed interaction site between GRO29A and the cellular protein(s) involves the core G-quartet region of the dimeric oligonucleotide structure. This is based on the structure–activity relationship we have developed with a number of substitutions in the G-quartet and loop regions. Therefore, a change in the structure of the G-quartet region should significantly alter the protein binding and antiproliferative activity. This is a possible explanation for the inability of MR29A to compete for protein and inhibit cell growth. Molecular modeling studies of GRO29A, MR29A, and MRdG29A demonstrated that the G-quartet regions are similar with respect to helical twist, rise, and sugar and phosphate backbone conformation, while the nature of the groove changes considerably depending on backbone type (Figure 5). These results indicate that oligonucleotide–protein interaction is highly selective and sensitive to change. Although, in this report, we did not specifically identify the protein which interacts with the oligonucleotides, there is evidence from our previous work that this protein is nucleolin (*14*). Nucleolin has previously been reported to bind to G-quartet sequences from telomeres (*41*), IgG switch regions (*5*, *42*) and ribosomal genes (*40*, *43*), as well as GRO29A (*14*), but its function as a G-quartet binding protein is not yet understood. The mechanism by which GRO29A binding to nucleolin can inhibit cell growth is still under investigation. The results presented in this report, however, confirm the importance of the specific G-rich oligonucleotide binding protein in the growth inhibitory properties of these oligonucleotides.

Our studies have also suggested that phosphodiester oligonucleotides may be the most useful backbone type for the development of therapeutic agents based on GRO29A. Although not generally considered to be suitable for in vivo use, due to their rapid degradation in serum, the stability of phosphodiester analogue of 29A is dramatically increased relative to that of non-G-quartet-forming oligonucleotides. This most likely reflects the very compact structure, which is assumed by these oligonucleotides, which is further stabilized by G-quartet formation.

Phosphorothioate oligonucleotides have been extensively tested in vivo and represent an alternative to phosphodiester ODNs. Even though PS29A has a similar efficacy compared to GRO29A, the phosphodiester molecule may have significant advantages over the phosphorothioate due to an expected decrease in nonspecific toxic side effects. The side effects seen with phosphorothioate oligonucleotides are most likely due to their polyanionic nature and their ability to stimulate the immune system (*17*). These toxicities are expected to be significantly reduced for phosphodiester oligonucleotides. The activity of the control phosphorothioate PS15B demonstrates that the mechanism of phosphorothioate effects may be very different (and less specific) from that of GRO29A.

Although full substitution of GRO29A with a 2′-*O*-methyl RNA backbone type abrogates antiproliferative activity, substitution of dT bases with 2′-*O*-methyluridine does not significantly reduce activity. Therefore, the mixed backbone oligonucleotide MRdG29A may also represent a promising molecule for therapeutic development.

While the exact mechanism of action of GRO29A and its analogues is still being investigated, it is likely that their growth inhibitory activity is related to their ability to bind one or more cellular proteins. It is clear that the ability of these oligonucleotides to form G-quartets and to bind to the cellular protein is related to their profound effects on cancer cell proliferation. It is important to stress that both of these characteristics are necessary for their activity but neither is sufficient by itself.

REFERENCES

1. Galderisi, U., Di Bernardo, G., Melone, M. A., Galano, G., Cascino, A., Giordano, A., and Cipollaro, M. (1999) *J. Cell. Biochem. 74*, 31–37.
2. Helene, C., Giovannangeli, C., Guieysse-Peugeot, A. L., and Praseuth, D. (1997) *CIBA Found. Symp. 209*, 94–102.
3. Burgess, T. L., Fisher, E. F., Ross, S. L., Bready, J. V., Qian, Y. X., Bayewitch, L. A., Cohen, A. M., Herrera, C. J., Hu, S. S., Kramer, T. B., et al. (1995) *Proc. Natl. Acad. Sci. U.S.A. 92*, 4051–4055.
4. Williamson, J. R. (1994) *Annu. Rev. Biophys. Biomol. Struct. 23*, 703–730.
5. Dempsey, L. A., Sun, H., Hanakahi, L. A., and Maizels, N. (1999) *J. Biol. Chem. 274*, 1066–1071.
6. Kettani, A., Kumar, R. A., and Patel, D. J. (1995) *J. Mol. Biol. 254*, 638–656.
7. Simonsson, T., Pecinka, P., and Kubista, M. (1998) *Nucleic Acids Res. 26*, 1167–1172.
8. Catasti, P., Chen, X., Moyzis, R. K., Bradbury, E. M., and Gupta, G. (1996) *J. Mol. Biol. 264*, 534–545.
9. Sun, D., Thompson, B., Cathers, B. E., Salazar, M., Kerwin, S. M., Trent, J. O., Jenkins, T. C., Neidle, S., and Hurley, L. H. (1997) *J. Med. Chem. 40*, 2113–2116.
10. Haq, I., Trent, J., Chowdhry, B., and Jenkins, T. (1999) *J. Am. Chem. Soc. 121*, 1768–1779.
11. Newbold, R. F. (1999) *Anticancer Drug Des. 14*, 349–354.
12. Lavelle, F., Riou, J. F., Laoui, A., and Mailliet, P. (2000) *Crit. Rev. Oncol. Hematol. 34*, 111–126.
13. Meeker, A. K., and Coffey, D. S. (1997) *Biochemistry (Moscow) 62*, 1323–1331.
14. Bates, P. J., Kahlon, J. B., Thomas, S. D., Trent, J. O., and Miller, D. M. (1999) *J. Biol. Chem. 274*, 26369–26377.
15. Xu, X., Hamhouyia, F., Thomas, S. D., Burke, T. J., Girvan, A. C., McGregor, W. G., Trent, J. O., Miller, D. M., and Bates, P. J. (2001) *J. Biol. Chem. 276*, 43221–43230.
16. Agrawal, S., and Crooke, S. T. (1998) *Antisense research and application*, Springer, Berlin and New York.
17. Agrawal, S. (1999) *Biochim. Biophys. Acta 1489*, 53–68.
18. Crooke, S. T. (1999) *Biochim. Biophys. Acta 1489*, 31–44.
19. Eckstein, F. (2000) *Antisense Nucleic Acid Drug Dev. 10*, 117–121.
20. Waters, J. S., Webb, A., Cunningham, D., Clarke, P. A., Raynaud, F., di Stefano, F., and Cotter, F. E. (2000) *J. Clin. Oncol. 18*, 1812–1823.

21. Yuen, A. R., Halsey, J., Fisher, G. A., Holmlund, J. T., Geary, R. S., Kwoh, T. J., Dorr, A., and Sikic, B. I. (1999) *Clin. Cancer Res. 5*, 3357−3363.
22. Cunningham, C., Holmlund, J., Schiller, J., Geary, R., Kwoh, T., Dorr, A., and Nemunaitis, J. (2000) *Clin. Cancer Res. 6*, 1626−1631.
23. Nemunaitis, J., Holmlund, J. T., Kraynak, M., Richards, D., Bruce, J., Ognoskie, N., Kwoh, T. J., Geary, R., Dorr, A., Von Hoff, D., and Eckhardt, S. G. (1999) *J. Clin. Oncol. 17*, 3586−3595.
24. Morgan, D. M. (1998) *Methods Mol. Biol. 79*, 179−183.
25. Ausubel, F. M. (1994) *Current protocols in molecular biology*, John Wiley & Sons, New York.
26. Wang, Y., and Patel, D. J. (1993) *Structure 1*, 263−282.
27. Mohamadi, F., Richards, N. G., Cuida, W. C., Liskamp, R., Lipton, M., Caufield, C., Chang, G., Hendricksen, T., and Still, W. C. (1990) *J. Comput. Chem. 11*, 440.
28. Nicholls, A., Sharp, K. A., and Honig, B. (1991) *Proteins 11*, 281−296.
29. Gao, D., and Trent, J. O. (2001) GrooveView: A computer program for quantitating groove shapes in multistranded DNA complexes.
30. Mergny, J. L., Phan, A. T., and Lacroix, L. (1998) *FEBS Lett. 435*, 74−78.
31. Giraldo, R., Suzuki, M., Chapman, L., and Rhodes, D. (1994) *Proc. Natl. Acad. Sci. U.S.A. 91*, 7658−7662.
32. Jing, N., Rando, R. F., Pommier, Y., and Hogan, M. E. (1997) *Biochemistry 36*, 12498−12505.
33. Bishop, J. S., Guy-Caffey, J. K., Ojwang, J. O., Smith, S. R., Hogan, M. E., Cossum, P. A., Rando, R. F., and Chaudhary, N. (1996) *J. Biol. Chem. 271*, 5698−5703.
34. Este, J. A., Cabrera, C., Schols, D., Cherepanov, P., Gutierrez, A., Witvrouw, M., Pannecouque, C., Debyser, Z., Rando, R. F., Clotet, B., Desmyter, J., and De Clercq, E. (1998) *Mol. Pharmacol. 53*, 340−345.
35. Marathias, V. M., and Bolton, P. H. (1999) *Biochemistry 38*, 4355−4364.
36. Cheng, A. J., Wang, J. C., and Van Dyke, M. W. (1998) *Antisense Nucleic Acid Drug Dev. 8*, 215−225.
37. Darnell, J. C., Jensen, K. B., Jin, P., Brown, V., Warren, S. T., and Darnell, R. B. (2001) *Cell 107*, 489−499.
38. Ramanathan, M., Lantz, M., MacGregor, R. D., Garovoy, M. R., and Hunt, C. A. (1994) *J. Biol. Chem. 269*, 24564−24574.
39. Bianchi, A., and de Lange, T. (1999) *J. Biol. Chem. 274*, 21223−21227.
40. Hanakahi, L. A., Sun, H., and Maizels, N. (1999) *J. Biol. Chem. 274*, 15908−15912.
41. Pollice, A., Zibella, M. P., Bilaud, T., Laroche, T., Pulitzer, J. F., and Gilson, E. (2000) *Biochem. Biophys. Res. Commun. 268*, 909−915.
42. Hanakahi, L. A., Dempsey, L. A., Li, M. J., and Maizels, N. (1997) *Proc. Natl. Acad. Sci. U.S.A. 94*, 3605−3610.
43. Ghisolfi, L., Joseph, G., Erard, M., Escoubas, J. M., Mathieu, C., and Amalric, F. (1990) *Mol. Biol. Rep. 14*, 113−114.

BI0119520